

The Collapse of the Beauvais Cathedral in 1284: The Conjecture of the Creep Buckling Piers

Mario Como

University of Rome "Tor Vergata", Rome, Italy

ABSTRACT: The paper analyzes the failure occurred at the cathedral of Beauvais in the past 1284. The interior vaulting exceeded 48 m in height, making it the tallest cathedral in Europe. The collapse was quite inexplicable and many theories have been debated trying to understand the reasons of the failure. This paper contributes to the discussion and investigates whether the creep buckling of the masonry piers could be considered responsible of the collapse. In this analysis the masonry has no tensile strength and the creep of the mortars is properly taken into account.

The study shows that the slenderness of the masonry piers, together with the eccentricities of the axial loads and the mortar's creep effects, can be considered the real causes of the failure.

INTRODUCTION

The cathedral of St Pierre at Beauvais, one of the most daring achievements of gothic architecture, consists only of a transept and a choir with apse and seven apse-chapels. The vaulting in the interior exceeds 48 m in height, to make it the tallest cathedral in Europe. The history of the construction of the cathedral is well known. (Branner 1962, pp. 78-92). The choir and the apse were started before 1245, and finished in 1272. The work was interrupted in 1284 by the collapse of the vaulting of the choir.

The works over the next 50 years included the construction of new piers with the span halved from about 9 m of the original length to 4.5 m. It was believed, in fact, that the original pier spacing of the failed choir was too large. The choir had been completely rebuilt by about 1337, though work was interrupted by the Hundred Years War. It was not until Sixteenth Century that the construction works started again. In 1573 the fall of an extremely high central tower stopped the work definitively. Beauvais became what it is today: a choir and transept without a nave.

The collapse which occurred in 1284 was quite inexplicable: the cathedral had stood in good conditions for twelve years and reports didn't register any earthquakes or wind storms before the collapse.

Many failure theories have been proposed. Many commentators blame the failure on the fact that the piers were too slender in relation to their height and to the load intensity. The fact that the cathedral collapsed after it had stood in good conditions for 12 years, according to Viollet-le Duc (1858-68, p.175) and to Heyman (1971, pp. 15-36; 1995, pp. 111-118), suggests that only a slow action could be the most probable cause of the failure. In this last conjecture, as Frankl (1962, p.101) suggests, the soil consolidation could have gradually produced increasing differential settlements and, thus, the failure. On the other hand, according to Wolfe and Mark comments (1976, pp.461-476), this conjecture seems unrealistic. The cathedral, in fact, was founded on the site of an earlier construction and closed within the walls of the old Roman precinct. Past excavations around the transept showed that the foundations were well built and the soil below was firm.

According to Viollet-le-Duc (ibidem), the creep of mortars could have produced load transfer from the masonry piers to the twin adjacent slender marble colonettes, shown under the statue in Fig. 1. As a consequence, the colonettes buckled, producing a rotation of the *tas de charge*, as well as a distortion of the adjacent flying buttress and the subsequent failure of vaults and piers. As it will be shown, taking into account the axial load eccentricities, the colonettes result unloaded: they are just decorative elements. Instead, for Mark

and Wolfe (ibidem), it was the complexity and the irregularity of the choir structure to be responsible of the failure because it had collected transversal thrusts. By photo elastic analysis high stresses were in fact evaluated in the piers. Also these last conclusions seem unlikely because based only on linear elastic evaluations. Then, which is the cause of the failure? Distance between main piers was about 15 m, the same of other cathedrals as Amiens, Chartres etc.. It was the height of the piers that, on the contrary, was greater than the others. According to Mark and Wolfe (ibidem, p.465), a very conservative analysis showed that the piers would not be able to buckle under the loadings conveyed from the original quadripartite vaults. This analysis seems too simply conducted, because founded only on the classical theory of stability of the elastic column. The complex geometry of the piers, with their offsets and misalignments, produced eccentricities of the axial loads. Thus, when the pier bends laterally, diffused cracks spread along its height, because the masonry no tensile strength. Strong stiffness reductions yield with further increase of bending: the pier can suddenly fail sideways. Yokel (1971, pp. 1913-1926) gave a clear evaluation of these effects in the column, assuming no tensile strength for the masonry material.

The only no tension assumption is, on the other hand, inadequate to explain the 1284 Beauvais failure, occurred twelve years after the completion of the vaults. Slow effects have to be considered in the pier stability analysis, taking into account masonry creep effects. According to many recent researches, creep of mortars can, in fact, produce remarkable additional strains (Jessop; Shrive; England, 1978, pp. 12.1-12.17)

FORCES ACTING ON THE PIERS

A preliminary static analysis of the cross vault, spanning the choir and the transept is firstly developed to evaluate the various actions conveyed to the piers. Fig. 4 shows a single bay of the quadripartite nave vault. The vault has been sliced into parallel arches supported by diagonal cross ribs.

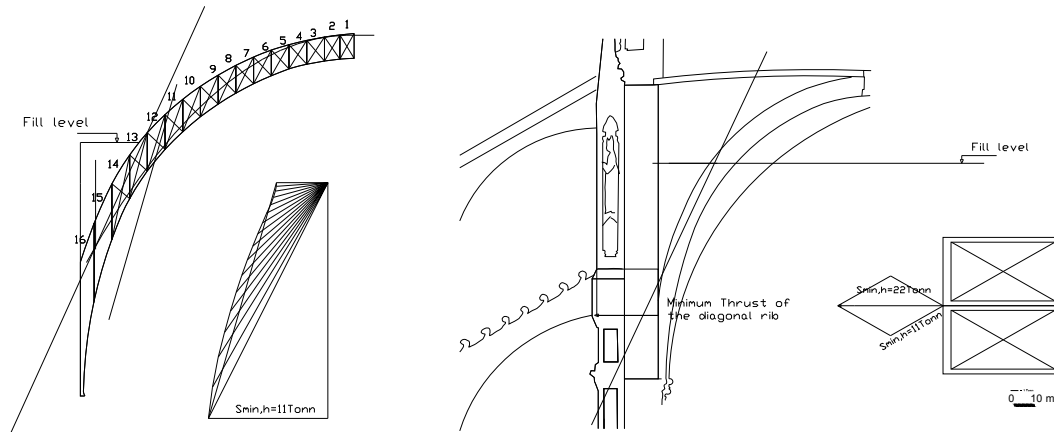


Figure 1: The minimum thrust conveyed by the diagonal cross ribs converging on the pier

The pressure line in the various sliced rings, together with their actions transmitted to the diagonal ribs, have been evaluated by the funicular polygon technique. (Fig.1). The cross rib is loaded by its weight and by the vertical and horizontal forces conveyed by the sliced arches. The small inflexions of vertical buttresses yield minimum thrust states in the sliced arches and into the ribs.

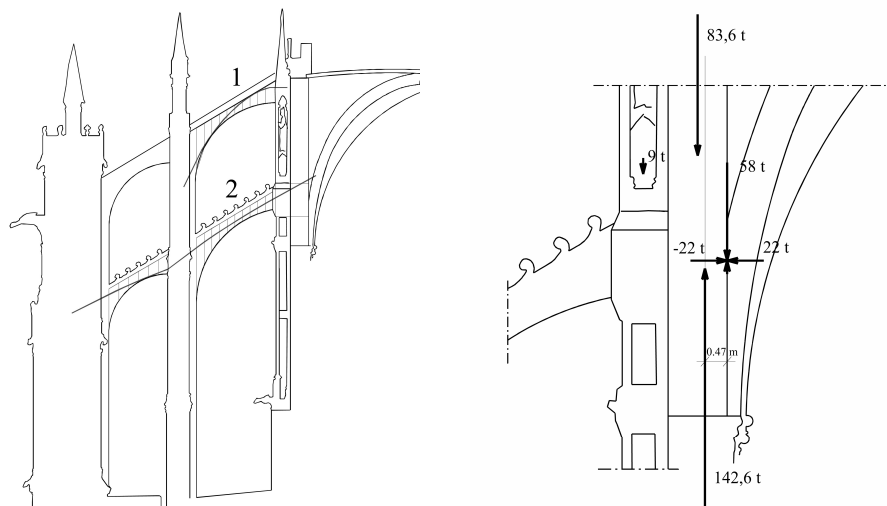


Figure 2 (left): Forces conveyed across the tas de charge
 Figure 3 (right): Lines of thrust in the flying buttresses

The pier height is of about 44,80 m, measured from the foundation level to the extrados of the *tas de charge*. The pier is here fixed because of the presence, on one side, of the flier and, on the other, of the springing of the nave cross vault. (Fig.4). Above the *tas de charge* the pier extends for about other 7 m, becoming part of the transversal upper walls. The total length of the pier is 44,80 + 7,00 = 51,80 m, of which about 3,80 m runs from foundation to floor levels. The examined length of the pier can be subdivided in two main segments. The lower, of the length of 25 m, has circular cross section with diameter of about 1,60 m and goes from the foundation level to the side vault extrados. The second segment of the pier, with length of 18 m, non-aligned against the first, reaches the intrados of the *tas de charge*. The section of this last pier segment, which is circular with a diameter of 1,25 m, is strengthened by four adjacent slender marble colonettes having a diameter of about 0,20 m, as shown in Fig. 5. All these measures are only approximate and have been obtained by inspection of the Benouville reconstruction of the original design for the choir of Beauvais (Benouville, 1891-2, pp. 52-54, 60-62, 68-70).

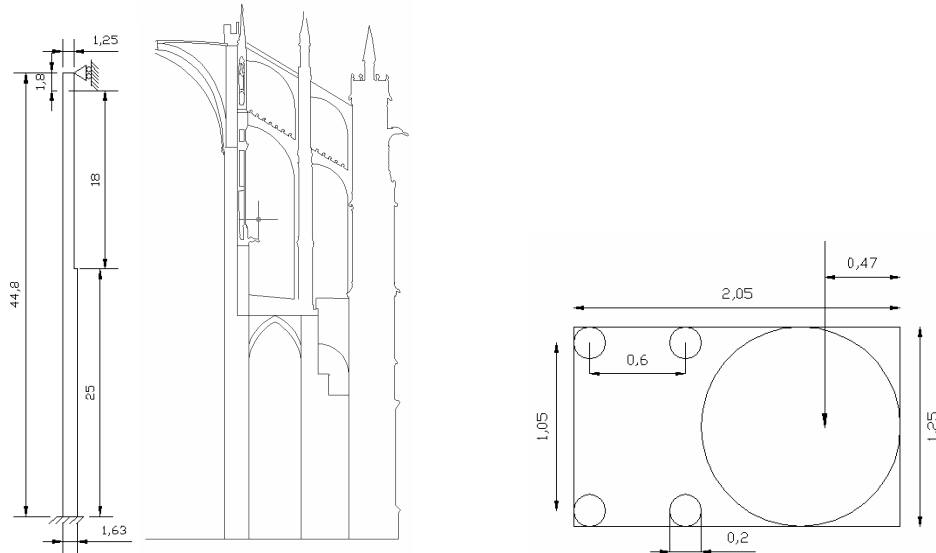


Figure 4 (left): Section at the transept with the pier; Figure 5 (right): Section of the upper length of the pier

The lower flier takes the horizontal component of the force S conveyed by the main vault. Only vertical loads act on the pier. These forces are specifically due to:

- 1) the weight of the roof and of the wooden trusses: considering, on average, a weight of 500 kg/m² in plan, we have: $W_{roof} = 9,00 \times 7,60 \times 0,5 = 34,20$ t applied along the axis of the masonry pier, at the distance of 0,625m from its internal edge.
- 2) the weight of the transverse masonry walls: considering an average area of 8,50 m X 9,00 m, a thickness of 0,4 mt, a reducing factor equal to 0,8, to take into account the presence of the openings, a specific gravity of 2 tons/mc, we have $W_{wall} = 9,00 \times 8,50 \times 0,40 \times 0,8 \times 2 = 48,9$ t. This force is applied along the pier axis, i.e., at the distance of 0,625m from its internal edge.
- 3) the weight of the marble statue placed on the extrados of the *tas de charge*. Approximately we have: $W_{statue} = 4$ t. This force acts at the distance $e = 1,65 - 0,625 = 1,025$ m from the centre of the pier cross section.
- 4) the weight of the external portion of the *tas de charge*, that is included between the external and the external edges of the pier: $W = 0,80 \times 1,05 \times 1,80 \times 2,5 = 3,8$ t
- 5) the weight of the pinnacle: $W_{pinn} = (\pi \times 1,0^2 / 3 \times 4) \times 3,0 \times 2,2 = 1,7$ t. Both these last forces act along the axis of the four marble columns, at the distance: $e = 2,05 - 0,40 - 0,625 = 1,025$ m from the centre of the pier section.
- 6) the vertical actions conveyed by the cross vault and by the lower flying buttress. The vault, at a state of minimum thrust, conveys a vertical force of 58 t; the vertical counterthrust of the lower flier is equal to 8 t. Consequently, $W_{vault} = 58,0 - 8,0 = 50$ t. This force acts at a distance of - 0,625 m from the centre of the section of the upper masonry pier.

The resultant: summing up all the above forces: $W_{tot} = 83,1 + 4 + 3,8 + 1,7 + 50 = 142,6$ t.

By evaluating the moment of all these forces around the centre of the pier section, the eccentricity e of the resultant force yields: $83,0 + (4 + 3,9 + 1,7) \times 1,025 - 50,0 \times 0,625 = 132,6$ ξ.

Hence $\xi = - 0,15$ m. The distance of W_{tot} from the internal edge of the pier at the extrados of the *tas de charge* is $e = 0,625 - 0,15 = 0,475$ m.

With this eccentricity the marble columns result to be unloaded, contrary to Viollet-le-Duc conjecture. Thus the eccentric axial load is sustained only by the circular masonry cross section of the pier. Finally, the side vault spanning the aisle conveys to the pier vertical and horizontal actions $V_2 = 21,0$ t; $H_2 = 4,8$ t.

These forces are applied at the intersection of the pier with the side vault, at the external edge of the pier section.

STABILITY ANALYSIS OF PIERS

Buckling of the eccentrically loaded masonry pier

Eccentric axial loads acting upon slender masonry piers produce high reductions of their axial strength. Yokel (ibidem) gives a clear evaluation of these effects in the elastic range, assuming no tensile strength for the masonry material. Let us consider, as an example, a masonry pier, with a rectangular cross section of height h , loaded by an axial force acting at distance u_1 from its external edge: we assume $u_1 > h/6$. When the pier bends laterally, a crack zone spreads along its height, because of the masonry no tensile strength. The stress distribution in the uncracked part of the cross sections is triangular. At the mid section and in the deformed pier configuration, let u_0 be the distance of the external edge of the pier from the axis of the load P . (Fig.6). According to Yokel (ibidem), by assuming no tensile strength, the relation connecting the axial load P with the transversal displacement u_0 at the pier mid section, in the case of $u_1 = t/3$, is

$$\frac{P}{P_{ec}} = \frac{4}{\pi^2} \alpha \sqrt{1-\alpha} + \alpha \left[\ln \left(\sqrt{\frac{1-\alpha}{\alpha}} + \sqrt{\frac{1}{\alpha}} \right) \right]^2 \quad \alpha = u_0 / u_1 \quad P_{ec} = \frac{9}{4} \cdot \frac{\pi^2 E b u_1^3}{h^2} \quad (1)$$

The curve plotted in Fig. 7 gives a graphical representation of equation (1). We notice the occurrence of a snapping failure under a critical load that can be dramatically reduced by increasing the load eccentricity.

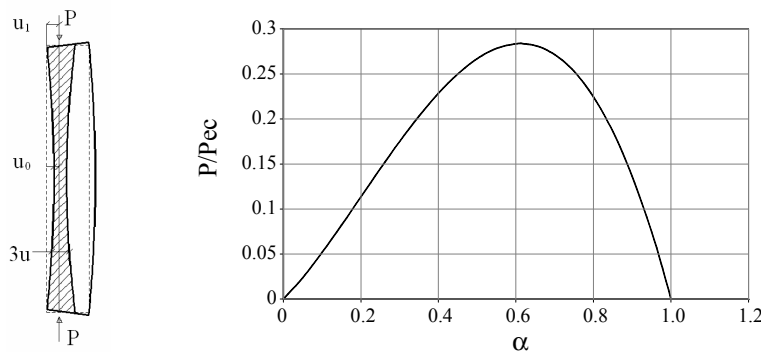


Figure 6 (left): The pier eccentrically loaded

Figure 7 (right): Axial load versus mid span lateral displacement

The masonry piers of the Beauvais cathedral are eccentrically loaded on the inner side by axial forces applied along their length. Additional eccentricity occurs at the level of the side-vault extrados because the offset occurring at that level in the pier axis.

Creep

Long term behavior of masonry materials has to be considered when evaluating the structural safety of historical buildings, especially when prone to destabilizing loads effects, as slender masonry piers and towers.

When a brickwork member is subjected to a sustained load, it undergoes an instantaneous elastic strain followed by a time dependent component, due to the creep mortars. The asymptotic creep strain can be even three-four times larger than the initial elastic strain (Jessop; Shrive; England, 1978, pp. 12.1-12.17).

The creep rate is quite rapid during the early stages of loading; then slows down gradually and it ceases after a period of time which varies from a few months to an year or more, providing that the stress level is well below the failure stress. On the removal of stress there is an instantaneous elastic recovery followed by a smaller delayed one; the pier is left with a permanent strain. If the pier is newly loaded, it will suffer the same process but with lower creep strains. This remark explains the longer duration of creep effects when a continuous modification of stress occurs during the time, due to coupling between geometrical and material non linearities. The sudden collapse of the tower of Pavia (1988) or the failure of the bell tower of San Marco in Venice (1892) are catastrophic examples of these effects. The creep of the mortars, particularly large in the old masonries for the thick joints, during the time produce pier flexure increments and, in turn, further increase the destabilizing effects of the axial loads. The viscous deformation of the masonry can be analyzed by means of the function $\Phi(t, \tau)$ which represents, at the present time t , the memory of the elastic strain occurred at the past time τ and lasted the unit time interval. The mortar has, approximately, indelible memory and we can assume

$$\Phi(t, \tau) = \alpha \beta e^{-\beta(\tau-t)} \quad (2)$$

where β is a constant of dimension $[t^{-1}]$, α is the viscosity factor, defining the intensity of the viscous strain, and t_0 the curing time of the mortar (Krall, 1947, pp. 47-55).

The test model of the creep buckling of the pier: comparisons with the delayed modulus approach

To explain the influence of the mortar creep on the stability of the masonry piers, it is useful to examine the response of the simplified model of visco-elastic no tension column of Fig. 8. Only the central voussoir is deformable and composed by a no tension visco-elastic material.

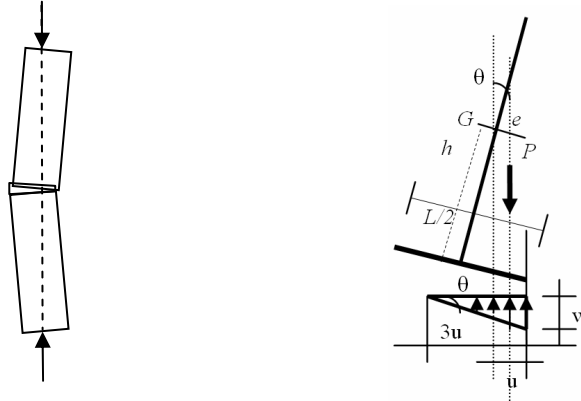


Figure 8 (left): The simplified model of the column; Figure 9 (right): Geometrical and mechanical quantities

Fig. 9 shows half column with the indication of all the various geometrical quantities involved. The column bends of a small angle θ under the action of the load P , applied at the centre G with eccentricity e and at the height h from the base of width L . The eccentricity of P at the base becomes $(e + h\theta)$ because of the rotation θ of the column. The distance u of the axis of P from the external side of the base section is

$$u = \left(\frac{L}{2} - e - h\theta\right) \quad (3)$$

By assuming at a first step that the central voussoir is made by a no tension elastic material,, with the assumption that $(L/2 - e - h\theta) > L/6$, the equilibrium equation of the column is

$$p = \frac{9}{2}(\gamma - \theta)^2 \theta, \quad p = \frac{P}{Eh^2}, \quad \gamma = \frac{L}{2h} - \frac{e}{h} \quad (4)$$

The critical equilibrium state is reached when

$$\frac{dP}{d\theta} = \frac{9}{2}kbh^2(\gamma - \theta)(-3\theta + \gamma) = 0 \quad (5)$$

With the mortar creep the equilibrium states of the pier gradually evolves. By using the memory function (2), the following equation controls the evolution of the column rotation during the time

$$3u(t)\theta(t) = \varepsilon_{tot}(t) = \left[\frac{2P}{3bEu(t)} + \alpha\beta \int_{t_1}^t e^{-\beta(\tau - t_o)} \frac{2P}{3bEu(\tau)} d\tau \right] \quad (6)$$

Substituting the expression (3) of the distance $u(t)$ into equation (6), we can easily obtain the following equation connecting the rotation $\theta(t)$ with the eccentric load P

$$\xi = 1 - \frac{9}{2} \frac{1}{\alpha p} \left[\gamma^2(\theta - \theta_o) - \frac{3}{2} \gamma(\theta^2 - \theta_o^2) + \frac{2}{3}(\theta^3 - \theta_o^3) \right] - \frac{1}{\alpha} \ln \frac{\gamma - \theta}{\gamma - \theta_o}, \quad \xi = e^{-\beta t} \quad (7)$$

and where, for sake of simplicity, we have assumed $t_o = t_1 = 0$. In equation (7) θ_o and $\theta(t)$ respectively indicate the rotation of the column at the initial time $t = 0$ and at time t . The column reaches the critical state when two different equilibrium configurations exist at the same time t , i.e. when, by using equation (7),

$$\frac{d\xi}{d\theta} = -2\theta_{cr}^3 + 5\gamma\theta_{cr}^2 - 4\gamma^2\theta_{cr} + \left(\gamma^3 - \frac{2}{9}p_{cr}\right) = 0 \quad (8)$$

The asymptotic rotation occurring when $t \rightarrow \infty$, i.e. for $\xi \rightarrow 0$, is indicated as θ_∞ . Thus, from equation (7), with $\xi = 0$ we have

$$0 = 1 - \frac{1}{\alpha} \frac{9}{2p} [\gamma^2(\theta_\infty - \theta_o) - \frac{3}{2} \gamma(\theta_\infty^2 - \theta_o^2) + \frac{2}{3}(\theta_\infty^3 - \theta_o^3)] - \frac{1}{\alpha} \ln \frac{\gamma - \theta_\infty}{\gamma - \theta_o} \quad (9)$$

From equation (10) it is possible to evaluate the asymptotic rotation θ_∞ due by the load P . The critical state is attained for $t \rightarrow \infty$ if the rotation $\theta = \theta_{cr,\infty}$ and the load $P_{cr,\infty}$ satisfy both equation (9) and (10), i.e.

$$-2\theta_{cr,\infty}^3 + 5\gamma\theta_{cr,\infty}^2 - 4\gamma^2\theta_{cr,\infty} + (\gamma^3 - \frac{2}{9}P_{cr,\infty}) = 0 \quad (8')$$

$$0 = 1 - \frac{1}{\alpha} \frac{9}{2p_{cr,\infty}} [\gamma^2(\theta_{cr,\infty} - \theta_o) - \frac{3}{2} \gamma(\theta_{cr,\infty}^2 - \theta_o^2) + \frac{2}{3}(\theta_{cr,\infty}^3 - \theta_o^3)] - \frac{1}{\alpha} \ln \frac{\gamma - \theta_{cr,\infty}}{\gamma - \theta_o} \quad (9')$$

In eq. (8') unknown quantities are $\theta_{cr,\infty}$ and $p_{cr,\infty}$ and in eq. (9') $\theta_{cr,\infty}$, θ_o and $p_{cr,\infty}$. The last equation requires from (5) the rotation θ_o occurring at $t = 0$ under $p_{cr,\infty}$: θ_o is thus given by

$$2/9 p_{cr,\infty} = (\gamma - \theta_o)^2 \theta_o \quad (5')$$

Substitution of (5') into equations (8') and (9') reduces the problem to the solution of a system of two equations in the unknowns $\theta_{cr,\infty}$ and θ_o for assigned values of the viscosity factor α . The asymptotic load $p_{cr,\infty}$ is then obtained, by equation, (5'). Tab.1 gives the values of x and x_o so defined

$$x_o = \theta_o / \gamma \quad x = \theta_{cr,\infty} / \gamma \quad (10)$$

Tab. 1: Solutions of equations (14) and (15) for assigned values of the viscosity factor α

α	x_o	X
0	1/3	1/3
1	0,102	0,390
2	0,067	0,415
3	0,050	0,430
4	0,040	0,441

Tab.2 gives the values of the asymptotic rotation $\theta_{cr,\infty}$ and of the initial rotation θ_o , together with the non dimensional load $p_{cr,\infty}$, corresponding to the above solutions x and x_o . The asymptotic critical loads $p_{cr,\infty}$, $p_{cr,\infty,del}$ can be approx. obtained by substitution into the expression (5) of the delayed elastic modulus

$$E = \frac{E}{1 + \alpha} \quad (11)$$

These values $p_{cr,\infty,del}$ are quoted in the last column of Tab.2. They represent approximate estimates of the critical load of the visco - elastic no tension model of the column.

Tab.2: Asymptotic critical loads corresponding to assigned values of viscosity factor α

α	$\theta_{cr,\infty}$	θ_o	$P_{cr,\infty}$	$P_{cr,\infty,del}$
1	0.390 γ	0.102 γ	0.370 γ^3	0.335 γ^3
2	0.415 γ	0.067 γ	0.262 γ^3	0.222 γ^3
3	0.430 γ	0.050 γ	0.203 γ^3	0.167 γ^3
4	0.441 γ	0.040 γ	0.166 γ^3	0.133 γ^3

These approximate values of $p_{cr,\infty,del}$ are always lower than the corresponding $p_{cr,\infty}$ but quite close to them.

This result can show that, in spite of the complexity of the problem, the delayed modulus critical loads can represent an approximate assessment of the effective critical loads. This result will be used to estimate the collapse load of the piers of the Beauvais cathedral.

Stability analysis of the Beauvais piers via delayed modulus approach

A non linear program Atena (Cervenka, 2002), able to take into account both the geometrical and mechanical non linearities, is used to analyze the stability of the cathedral piers. On the basis of the previous assessments, the effects of the masonry creep are analyzed by means of the simplified delayed elastic modulus approach. The more complex geometry of the Beauvais piers (Fig. 4) has been introduced into the program Atena in a bi-dimensional form.

Because of the eccentricity of the axial load, the slender marble columns adjacent to the masonry pier, are unloaded and have not been taken into account. The pier is loaded at its upper section by an axial load $P = 142$ tons with the eccentricity $e = 0.47$ m, and by the others loads applied along its length. The program includes automatically the weight of the various pier segments. All the loads are affected by the parameter λ , variable in the interval (0,1), so that the effective loads are in action when λ reaches the unity. The horizontal displacement Δ of the pier is evaluated at the level of the side vault extrados, where the pier section changes width. Different curves axial load versus lateral displacement Δ have been plotted by gradually increasing λ and for different values of the delayed elastic modulus (Fig.10).

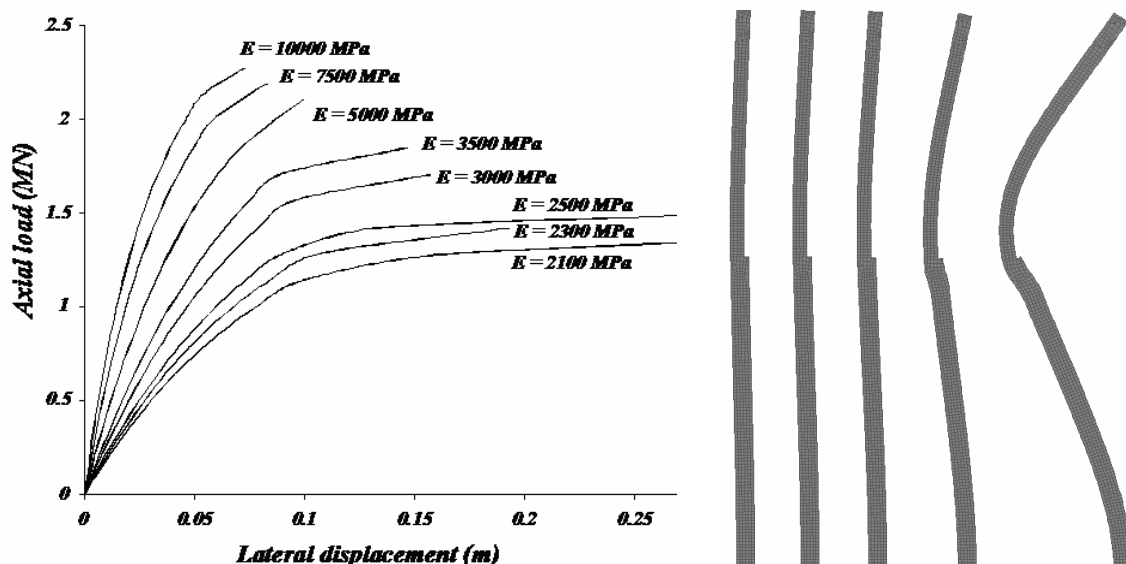


Figure 10 (left): Axial load–lateral displacement curves by reducing the delayed Modulus
 Figure 11 (right): Pier inflexions under full loading and $E = 10000, 7500, 5000, 3500, 2100$ MPA

Because of the long term creep effects in the mortars, the delayed modulus can be assumed lower up to four times the initial value E . Taking into account the order of magnitude of the initial elastic modulus, ranging between 10000 MPa - 5000 MPa and the corresponding decays due to creep effects, the behavior of the pier is strongly unstable. We notice that, if the modulus is near to its initial value, the pier can fail only under loads much larger than the real ones. On the contrary, for values of the delayed modulus that take into account the creep effect, the pier has a delayed failure under its ordinary loads. Numerical calculations also show that small variations of the loads or of their eccentricities produce small changes of the pier response.

Fig.11 gives a representation of the different inflexions of the pier, under the full load action, by gradually releasing the delayed masonry modulus.

CONCLUSIONS

The slenderness of the masonry piers, with their axis non alignments and the eccentric loads, together with the presence of the mortar creep, can be responsible of the past failure occurred in the year 1284. In spite of all these eccentricities and the destabilizing effect of the axial loads, piers are initially stable. The creep deformations of the medieval mortars, on the other hand, gradually increase the pier inflexion during time. The creep effects, intensifying the destabilizing action of the axial loads, slowly move the pier towards more precarious equilibrium states up to the disastrous collapse.

In conclusion, the 1284 Beauvais failure can be due to the creep buckling of masonry piers.

REFERENCES

- Benouville, L. 1891-1892: Etude sur la Cathédrale de Beauvais, *Encyclopédie d'Architecture*, S. 4,4, Paris pp.52-54, 60-62, 68-70.
- Branner, R., 1962: Le Maître de la Cathédrale de Beauvais *Art de France*, 2, Paris, pp. 77-92.
- Frankl, P., 1962: *Gothic Architecture*, London, p.101.
- Heyman, J. 1971: Beauvais Cathedral, *Transactions of the Newcomen Society*, 40, 1967-1968, London, pp.15-36.
- Heyman, J. 1995: *The Stone Skeleton*, Cambridge University Press, 1995 pp.111-118.
- Jessop, E.L.; Shrive, N.G.; England G. L., 1978: *Elastic and Creep Properties of Masonry*, Proceedings of the North American Masonry Conference, The masonry Society, pp. 12.1-12.17.
- Viollet-le-Duc, E.E., 1858-1868: Dictionnaire raisonné de l'architecture française du XI^e au XVI^e Siècle, 10 vols. Paris, 4, p.78.
- Wolfe M.I., Mark, R., 1976: The collapse of the vaults of the Beauvais Cathedral in 1284, *Speculum*, Vol. 51, n.3, Medieval Academy of America, pp. 462 - 476.
- Yokel F.Y., 1971: Stability and load capacity of members with no tensile strength, *Proc. ASCE*, 97 ST7, pp.1913 - 1926.
- Krall, G.; 1947, Statica dei mezzi elastici cosiddetti viscosi e sue applicazioni, *Rend. Acc. Naz.le dei Lincei*, fasc. 3-4, Roma, pp. 47-55.
- Cervenka, V. and J. , 2002, Atena Program Documentation, User's manual, Prague.